Electronic coupling in organic-inorganic semiconductor hybrid structures with type-II energy level alignment

S. Blumstengel,* S. Sadofev, C. Xu, J. Puls, R. L. Johnson,† H. Glowatzki, N. Koch, and F. Henneberger
Institut für Physik, Humboldt-Universität zu Berlin, Newtonstrasse 15, 12489 Berlin, Germany
(Received 12 November 2007; revised manuscript received 19 December 2007; published 27 February 2008)

Electronic coupling in a hybrid structure made of ZnMgO and a spirobifluorene derivative (SP6) is investigated in the situation where the energy level alignment at the organic/inorganic interface revealed by photoelectron spectroscopy is of type II. Charge separation caused by electron transfer from the SP6 lowest unoccupied molecular orbital to the conduction band of the semiconductor is observed. By collecting the photogenerated carriers in a ZnO quantum well, very efficient exciton transfer from the inorganic to the organic part occurs as well.

DOI: 10.1103/PhysRevB.77.085323 PACS number(s): 81.07.Pr, 78.67.−n, 79.60.Jv

I. INTRODUCTION

Integration of organic and inorganic semiconductors in a hybrid structure is a promising way to exploit favorable properties of both material classes and to achieve novel photonic properties.[1] As a precondition, efficient electronic coupling across the organic/inorganic interface is required. Recently, we have shown that ZnO/ZnMgO quantum well (QW) excitons can be efficiently transferred to an organic overlayer of the blue emitting dye 2,2′-p-phenylene bis(5-phenyloxazol) (POPOP) by a dipole-dipole-mediated energy transfer step.[2] Meanwhile, similar findings have been reported on polymer-InGaN/GaN (Ref. 3) and J-aggregate-nanocrystal hybrid systems.[4] In this work, we address the situation where the energy level alignment between the organic and inorganic components is of type II. It is realized when ZnO or ZnMgO is combined with a spirobifluorene derivative. Specifically, both the energies of the highest occupied molecular orbital (HOMO) and lowest unoccupied molecular orbital (LUMO) are larger than the valence band maximum (VBM) and the conduction band minimum (CBM) of the semiconductor, respectively. Charge separation at the organic/inorganic interface as a central step for photovoltaic applications is demonstrated. Incorporation of a QW collecting the carriers photoexcited in the inorganic semiconductor allows for avoidance of charge separation and the occurrence of exciton transfer to the organic layer.

II. EXPERIMENT

A. Growth of hybrid structures

The hybrid structures were grown under ultrahigh vacuum conditions by molecular beam exitaxy in a DCA 450 double-chamber apparatus. In this way, the organic layer is deposited on a pristine and single-crystalline semiconductor surface. The inorganic part is made of ZnMgO epilayers or ZnO/ZnMgO QW structures, the MBE growth of which is described in detail elsewhere.[5] As substrate, *a*-plane sapphire is used, which induces growth along the *c* axis of the wurtzite crystal, resulting in the O-terminated $(000\bar{1})$ surface. ZnO as well as ZnMgO exhibit robust surface reconstructions enabling the preparation of well-defined interfaces free of defect states acting as quenchers.[2,5] The band gaps covered by ZnMgO extend from 3.3 to 4.4 eV and predestines such heterostructures for various optoelectronic applications in the ultraviolet spectral range. 2,7-bis(biphenyl-4-yl)-2′,7′-di-tert-butyl-9,9′-spirobifluorene (SP6) was purchased from Merck and used without further purification. The chemical structure is given in Fig. 1(a). The spiro linkage of SP6 prevents crystallization[6] and the deposited molecules form, thus, an amorphous layer. This is demonstrated by the atomic-force micrograph (AFM) of SP6 on $Zn_{0.86}Mg_{0.14}O$ $(000\bar{1})$ taken in tapping mode [Fig. 1(b)]. The thickness of the SP6 layer is $d_{SP6}=2.2$ nm as measured by a quartz microbalance. Its morphology follows exactly that of the ZnMgO surface. The steps in the height profile [Fig. 1(c)] correspond to monolayer or double layer steps of the wurtzite lattice ($c=0.519$ nm). When mechanical force is applied to the organic film with the AFM tip operated in hard tapping mode, the layer breaks up as seen in the 1×1 μm^2 square in the center of the image of Fig. 1(b). This confirms that SP6 is, indeed, present on the ZnMgO surface and that even the first few layers form homogeneous smooth films which are essential for the following investigations.

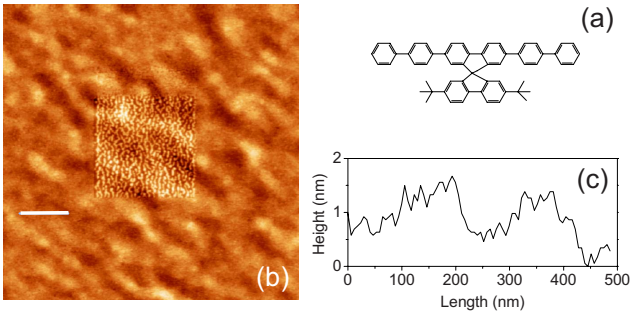

FIG. 1. (Color online) (a) Chemical structure of SP6. (b) AFM image of SP6 ($d_{SP6}=2.2$ nm) on ZnMgO $(000\bar{1})$. The deposition rate is 0.1 nm/min and the substrate temperature is 20 °C. (c) Height profile taken along the white line in the AFM image.

B. Characterization

The electronic structure of the interface and the energy offsets between the VBM of the inorganics and the HOMO of the organics $\Delta E_{\mathrm{VBM/HOMO}}=E_{\mathrm{VBM}}-E_{\mathrm{HOMO}}$ were determined by ultraviolet photoelectron (UP) spectroscopy. The measurements were performed at the FLIPPER II endstation at HASYLAB (Hamburg, Germany) in an analysis-preparation chamber tandem with base pressures of 4×10^{-10} and 5×10^{-9} mbar, respectively. The spectra were recorded with a double-pass cylindrical mirror analyzer at a photon energy of 22 eV. For measuring the secondary electron cutoff, a sample bias of −6 V was applied. SP6 is deposited both on a ZnO $(000\bar{1})$ single crystal (Crystec) as well as on a $Zn_{0.86}Mg_{0.14}O$ $(000\bar{1})$ epilayer. Prior to deposition of the organic layer, ZnO and ZnMgO surfaces were treated by repeated Ar-ion sputtering and annealing cycles. UP spectra were obtained for stepwise increasing thickness of the SP6 layer up to 3.2 nm.

Charge separation and excitation energy transfer across the organic/inorganic interface were studied by cw and time-resolved photoluminescence (PL) spectroscopy. PL transients were measured by time-correlated single-photon counting with a resolution of 10 ps. The excitation pulses were delivered by the frequency doubled output of a synchronously pumped dye laser, and spectral selectivity is provided by a double monochromator in subtractive mode with a resolution of 0.4 nm. PL and PL excitation (PLE) spectra were measured using a Xe lamp with the excitation wavelength selected by a double monochromator. The PL was recorded with a photomultiplier after passing a monochromator.

III. RESULTS AND DISCUSSION

A. Interfacial electronic structure

The valence electron photoemission spectrum of ZnO $(000\bar{1})$ [bottom curve in Fig. 2(a)] shows an energy separation between the VBM at the surface and the Fermi energy (E_F) of 2.50 eV. The feature at 4.2 eV is related to the O $2p$ orbital.[7] Upon deposition of SP6, the photoemission intensity from ZnO is attenuated and distinct features attributed to SP6 molecular orbitals become visible. At a nominal thickness of 0.8 nm, they dominate the spectra. The top spectrum is a simulated photoemission spectrum of SP6 obtained by Gaussian broadening (full width at half maximum of 0.7 eV) of the molecular eigenenergies obtained by semiempirical AM1 calculations using the CACHE software provided by Fujitsu, Inc. It reproduces the experimental data well. The levels of SP6 do not shift in energy with increasing thickness and also the shape remains the same, indicating that band bending in the organic layer is absent and that the electronic structure of the molecules does not change upon adsorption on ZnO. The molecules are, thus, bound by van der Waals interaction only. This finding is in contrast to other semiconductor surfaces on which chemical bond formation or even fragmentation of deposited molecules was observed.[8,9] The binding energy onset of the SP6 HOMO is 1.70 eV below E_F, from which the value $\Delta E_{\mathrm{VBM/HOMO}}=-0.80$ eV follows

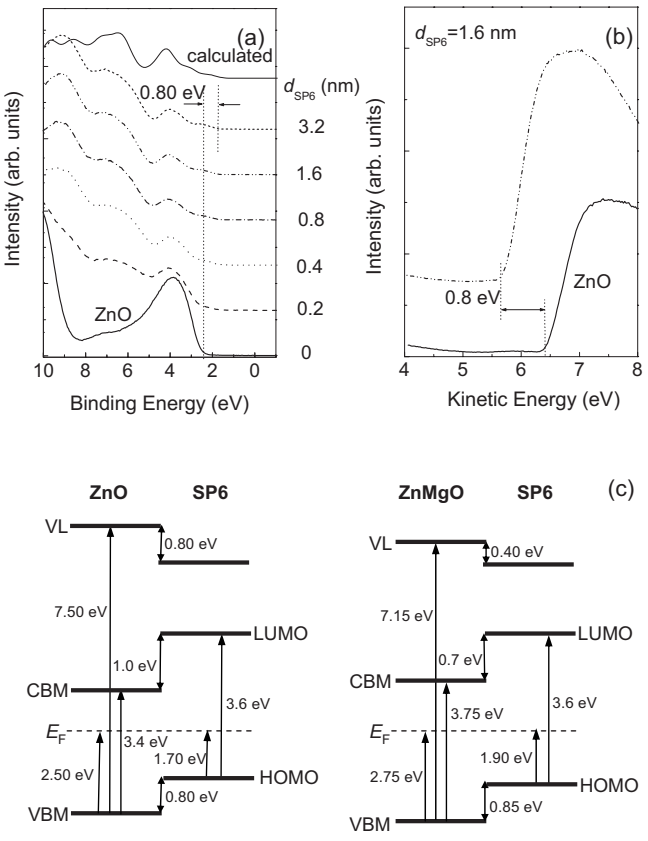

FIG. 2. (a) Valence region photoemission spectra of ZnO (solid line) and ZnO/SP6 for increasing thicknesses of SP6. (b) Secondary electron cutoff for pristine ZnO (solid line) and ZnO covered with 1.6 nm SP6 (dashed dotted line). (c) Energy level diagram of SP6/ZnO and SP6/ZnMgO interfaces. The experimental accuracy of the photoemission data is ±50 meV. The exciton binding energy of ZnO and ZnMgO is taken as 60 meV (Ref. 13), while that of SP6 is assumed to be similar to the value of 0.45 eV reported for a ladder-type poly(para-phenylene) (Ref. 14). VL: vacuum level.

for the SP6/ZnO heterointerface. The shift of the secondary electron cutoff from 6.4 to 5.6 eV [Fig. 2(b)] represents the reduction of the work function of ZnO caused by deposition of SP6, likely associated with a modification of the surface dipole and the electron-density distribution on the ZnO $(000\bar{1})$ surface. Analogous examples exist for organic/metal and other organic/inorganic semiconductor interfaces.[10–12] The valence electron photoemission spectra of the SP6/$Zn_{0.86}Mg_{0.14}O$ $(000\bar{1})$ interface formation are qualitatively identical with those of ZnO and are, therefore, not depicted. The data yield a slightly larger energy offset $\Delta E_{\mathrm{VBM/HOMO}}=-0.85$ eV. The position of the vacuum level, i.e., the work function, decreases only by 0.4 eV.

The CBM-LUMO offset $\Delta E_{\mathrm{CBM/LUMO}}=E_{\mathrm{CBM}}-E_{\mathrm{LUMO}}$ is easily calculated by adding to E_{VBM} and E_{HOMO} the optical band gaps, obtained from absorption measurements, and the exciton binding energies of the respective component. The resultant energy schematics are represented in Fig. 2(c). Both, for SP6/ZnO ($\Delta E_{\mathrm{CBM/LUMO}}=-1.0$ eV) as well as SP6/ZnMgO ($\Delta E_{\mathrm{CBM/LUMO}}=-0.7$ eV), CBM-LUMO offsets are

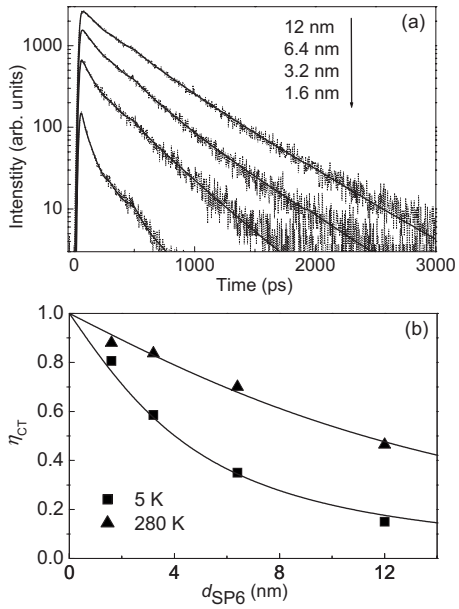

FIG. 3. (a) SP6 PL transients at 5 K of SP6/ZnMgO hybrid structures for increasing thicknesses of the organic layer. The excitation energy is set below the absorption edge of ZnMgO at $E_{ex}=3.59$ eV. (b) Dependence of the charge transfer efficiency η_{CT} on the layer thickness d_{SP6} at 5 K (■) and 290 K (▲). The solid lines are fits as explained in the text.

negative. Consequently, both configurations form type-II heterointerfaces, facilitating charge separation with the electron in the semiconductor and the hole in SP6. In what follows, the relevant transfer processes in the hybrid structures are studied by optical spectroscopy.

B. Charge separation

The charge separation process is most easily studied by exciting a SP6/ZnMgO hybrid structure below the ZnMgO band gap so that only excitons in the molecular layer are generated initially. Subsequent charge separation via electron transfer from the SP6 LUMO to the ZnMgO conduction band will show up in a quenching of the PL yield and a shortening of the lifetime. The degree to which this happens depends on how many of the excitons created in the SP6 film do reach the interface before they radiatively recombine. The PL decay of SP6 on $Zn_{0.86}Mg_{0.14}O$ (thickness of 600 nm) is depicted in Fig. 3. The observed shortening of the SP6 PL lifetime with decreasing layer thickness $d_{SP6}=1.6-12$ nm is in full agreement with the above described scenario. The efficiency of the charge transfer (CT) process given by $\eta_{CT}=(I_0-I_{HB})/I_0$, with I_{HB} and I_0 being the SP6 PL yield of the hybrid structures and on an inert quartz substrate, respectively, is obtained by integrating the normalized PL transients after deconvolution with the system response. The resultant η_{CT} as a function of d_{SP6} is depicted in Fig. 3(b). Exciton diffusion in the organic layer is described by the one-dimensional diffusion equation, whereby charge separation at the SP6/ZnMgO interface is taken into account by the boundary condition $D\mathrm{d}n(x=d_{SP6})/\mathrm{d}x=-sn$. n is the volume density of SP6 Frenkel excitons, D the diffusion constant, and s the surface recombination velocity with which excitons are removed via dissociation. Quenching at the SP6 surface is neglected, yielding $\mathrm{d}n(x=0)/\mathrm{d}x=0$. Using the standard steady-state solution and calculating the PL yield by integration of $n(x)$ over the layer thickness provide the data fits shown in Fig. 3(b). With an absorption coefficient $\alpha_{SP6}=4\times10^5$ cm^{-1} inserted in the generation term and a PL lifetime of SP6 $\tau_0=300$ ps in the recombination term, the fits yield estimates for $s\approx2000$ cm/s (5 K) and $s\approx5500$ cm/s (300 K) as well as for the diffusion length $L_D=\sqrt{D\tau_0}\approx3.7$ nm (5 K) and $L_D\approx10$ nm (300 K) of SP6 Frenkel excitons. As $L_D/2<s\tau_0$, the rate limiting step in the investigated configuration is diffusion of excitons toward the heterointerface. For reasonable distances d between the molecules and the ZnMgO surface, i.e., distances well above the van der Waals radius, d/s yields transfer times that can become as small as 10 ps. The strong thickness dependence of η_{CT} results from the small exciton diffusion lengths in the amorphous material. Charge separation through hole transfer from the semiconductor to SP6 is more difficult to evaluate in a similarly designed experiment as band bending at the semiconductor surface may also influence the ZnMgO PL yield and lifetime. It is, however, possible to inhibit hole transfer by introduction of a ZnO QW, which acts as a collector for electrons and holes photogenerated in the ZnMgO barrier. If this QW is close enough to the organic interface (~2–10 nm), efficient exciton transfer to SP6 is observed as detailed in the next section.

C. Excitation energy transfer

To quantify efficiency and time scale of the energy transfer process, hybrid structures consisting of $ZnO/Zn_{0.86}Mg_{0.14}O$ $(000\bar{1})$ QWs covered with a thin layer of SP6 are prepared. The ZnO/ZnMgO QW structure is composed of a 600-nm-thick ZnMgO barrier layer on which the ZnO QW is deposited. The QW is capped with a ZnMgO barrier layer of variable thickness $L_S=2-7.5$ nm. The well thickness $d_{QW}=3.5$ nm ensures in conjunction with the chosen Mg content in the barriers robust charge carrier confinement in the ZnO QW. On top of the upper ZnMgO barrier, the SP6 layer with 2.2 nm thickness is deposited. Figure 4(a) compares the PL spectrum of a ZnO/ZnMgO reference sample with the PLE spectrum of SP6 deposited on sapphire. The PL spectrum of SP6 on sapphire is shown as well. As there is spectral overlap between the ZnO QW as well as the ZnMgO barrier layer PL and the S_1 absorption band of SP6, excitation energy transfer is expected to occur from the inorganic to the organic part of the hybrid structure. This is, indeed, the case as evidenced by the observation of the prominent ZnO QW and ZnMgO barrier absorption features in the PLE spectrum of SP6 in the hybrid structure depicted in Fig. 4(b). For comparison, the QW PLE spectrum of the hybrid structure is shown as well. It reveals the substructure of the valence band as well as the ZnMgO barrier band edge, the latter being indicative of efficient carrier capture by the ZnO QW. According to the energy level alignment at the interface, there is an energetic barrier inhibiting the transfer

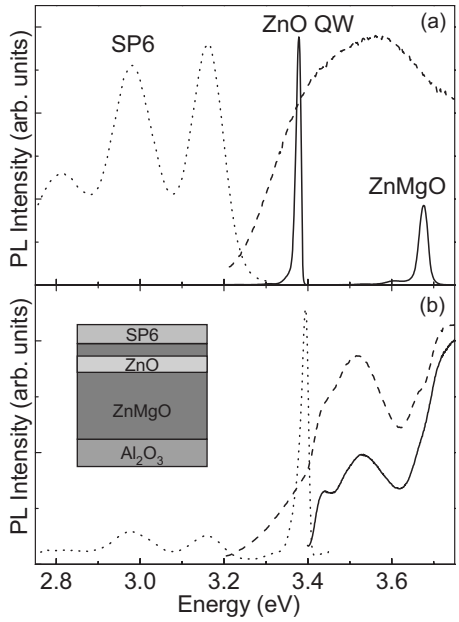

FIG. 4. (a) Reference samples: PLE (dashed line) and PL (dotted line) spectra of SP6 on sapphire and PL spectrum of a ZnO/ZnMgO QW structure with L_S=5 nm (solid line). (b) SP6/ZnO/ZnMgO hybrid structure with L_S=2 nm: PLE of the ZnO QW measured at E_{em}=3.35 eV (solid line), PLE of SP6 measured at E_{em}=2.95 eV (dashed line), and PL spectrum of the hybrid structure excited at E_{ex}=3.7 eV (dotted line). The inset shows schematically the design of the hybrid structure. All measurements were performed at 5 K.

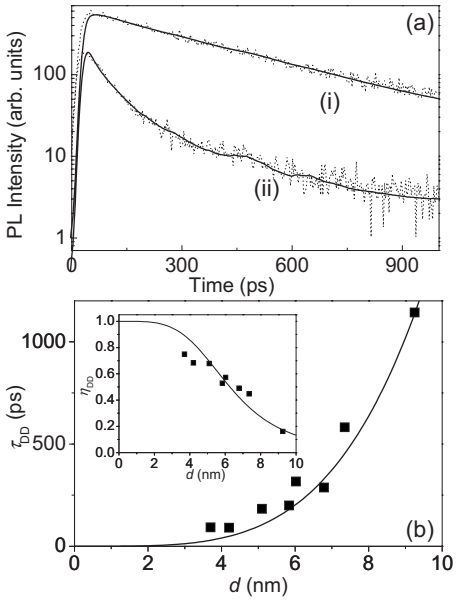

FIG. 5. (a) QW PL transients of a ZnO/ZnMgO reference sample (i) with L_S=2 nm and (ii) the hybrid structure of Fig. 4(b) obtained by exciting the samples at E_{ex}=3.97 eV. The temperature is 5 K. The decay curves were convoluted with the system response using an exponential law (solid lines). (b) τ_{DD} and η_{DD} (inset) as function of the distance $d=L_S+d_{QW}/2$. The solid lines are fits as explained in the text.

of electrons from the ZnMgO conduction band to the SP6 LUMO level. Consequently, separate injection of electrons and holes into the organic layer cannot contribute to the enhancement of the SP6 PL yield in the spectral region where the ZnO QW and ZnMgO barrier absorb. The nonradiative character of the energy transfer process is demonstrated by the shortening of the QW PL lifetime upon deposition of SP6, see Fig. 5(a). The lifetime of the QW excitons decreases from τ_{QW}=275 ps obtained for the ZnO/ZnMgO reference sample to τ_{HB}=69 ps in the SP6/ZnO/ZnMgO hybrid structure. This yields an energy transfer time of $\tau_{DD}=(1/\tau_{HB}-1/\tau_{QW})^{-1}$=92 ps and an efficiency $\eta_{DD}=1-(\tau_{HB}/\tau_{DD})$ =0.75. That means that three out of four excitons generated in the ZnO QW are transferred to the organic overlayer, generating SP6 Frenkel excitons. This efficiency is even higher than that of POPOP/ZnO/ZnMgO hybrid structures (η_{DD} =0.5 and R_0=3.5 nm),[2] which is in agreement with the larger Förster radius R_0=3.9 nm for the SP6/ZnO/ZnMgO structures as calculated from the spectral overlap integral. The efficiency η_{DD} decreases with increasing distance d between QW and organic layer [inset of Fig. 5(b)]. For a dipole-dipole-mediated transfer process in the present two-dimensional setting, the energy transfer time depends on the distance d between donor and acceptor as $\tau_{DD}^{-1}=(1/2)\tau_{QW}^{-1}N(R_0/d)^4$, with N being the number of molecules in the Förster cycle. The experimental data follow well the d^4 dependence, see Fig. 5(b). The fit yields, moreover, R_0 =3.1 nm, in fair agreement with the calculated value.

Finally, one can compare the efficiencies of electron and exciton transfer across the organic/inorganic interface for a given sample geometry. In the frame of the diffusion treatment, exciton transfer is represented by a positive flux $j_{ET}=G_0\eta_{DD}A_{QW}$ which has to be added to the surface recombination flux $j_{SR}=-sn$ at the organic/inorganic interface approximated in lowest order by $-G_0 s\alpha_{SP6}\tau_0$. G_0 is the incident photon pump flux. At a given transfer efficiency η_{DD}=0.75 (L_S=2 nm), the net outcome is controlled by the exciton fraction A_{QW} generated per incident photon in the QW. For optical excitation into the ZnMgO barrier, $A_{QW}\approx 0.5$, resulting in a positive total flux, while for direct excitation of the ZnO QW, $A_{QW}\approx 0.1^2$ yields $j_{ET}<j_{SR}$.

IV. CONCLUSIONS

In agreement with the energy level alignment derived by UP spectroscopy, excitons are dissociated efficiently via charge separation at the SP6/ZnMgO interface. On the other hand, if a ZnO QW is embedded into ZnMgO close to the organic interface, we observe exciton transfer with an efficiency of up to 75% from the QW to SP6. The measured distance dependence of the transfer rate corroborates our assumption that the coupling between Frenkel and Wannier excitons is mediated via dipole-dipole interaction. These findings show very clearly that despite the very different nature of organic and inorganic semiconductor materials, the interface between them is electronically active. In particular, defect states that might trap the carriers and impede both

charge and energy transfer across the interface play obviously no essential role. Moreover, the versatility of organic/inorganic hybrid structures for use in optoelectronic applications, such as light-emitting diodes, photodiodes or photovoltaic cells benefiting from the easy tunability of absorption and emission as well as large light-matter interaction cross sections of the organics and the favorable charge transport properties of the inorganics, is demonstrated as a step toward practical devices with optimized material combinations and geometries.

ACKNOWLEDGMENTS

The authors thank J. P. Rabe for the use of the AFM. Financial support by the DFG in frame of Sfb 448 is acknowledged. N.K. acknowledges financial support by the Emmy Noether-Program (DFG).

*sylke.blumstengel@physik.hu-berlin.de
†Institut für Experimentalphysik, Universität Hamburg, 22761 Hamburg, Germany.

[1] V. M. Agranovich, D. M. Basko, G. C. La Rocca, and F. Bassani, J. Phys.: Condens. Matter **10**, 9369 (1998).
[2] S. Blumstengel, S. Sadofev, C. Xu, J. Puls, and F. Henneberger, Phys. Rev. Lett. **97**, 237401 (2006).
[3] G. Itskos, G. Heliotis, P. G. Lagoudakis, J. M. Lupton, N. P. Barradas, E. Alves, S. Pereira, I. M. Watson, M. D. Dawson, J. Feldmann, R. Murray, and D. D. C. Bradley, Phys. Rev. B **76**, 035344 (2007).
[4] Q. Zhang, T. Atay, J. R. Tischler, M. S. Bradley, V. Bulovic, and A. V. Nurmikko, Nat. Nanotechnol. **2**, 555 (2007).
[5] S. Sadofev, S. Blumstengel, J. Cui, J. Puls, S. Rogaschewski, P. Schäfer, Y. G. Sadofyev, and F. Henneberger, Appl. Phys. Lett. **87**, 091903 (2005).
[6] N. Johansson, J. Salbeck, J. Bauer, F. Weissortel, P. Broms, A. Andersson, and W. R. Salaneck, Adv. Mater. (Weinheim, Ger.) **10**, 1136 (1998).
[7] R. T. Girard, O. Tjernberg, G. Chiaia, S. Soderholm, U. O. Karlsson, C. Wigren, H. Nylen, and I. Lindau, Surf. Sci. **373**, 409 (1997).
[8] G. Hughes, J. Roche, D. Carty, T. Cafolla, and K. E. Smith, J. Vac. Sci. Technol. B **20**, 1620 (2002).
[9] R. Lin, M. Galili, U. J. Quaade, M. Brandbyge, T. Bjørnholm, A. Degli Esposti, and F. Biscarini, J. Chem. Phys. **117**, 321 (2002).
[10] H. Ishii, K. Sugiyama, E. Ito, and K. Seki, Adv. Mater. (Weinheim, Ger.) **11**, 605 (1999).
[11] A. Kahn, N. Koch, and W. Gao, J. Polym. Sci., Part B: Polym. Phys. **41**, 2529 (2003).
[12] S. Blumstengel, N. Koch, S. Duhm, H. Glowatzky, R. L. Johnson, C. Xu, A. Yassar, J. P. Rabe, and F. Henneberger, Phys. Rev. B **73**, 165323 (2006).
[13] K. Hümmer, Phys. Status Solidi B **56**, 249 (1973).
[14] M. Kemerink, S. F. Alvarado, P. Muller, P. M. Koenraad, H. W. M. Salemink, J. H. Wolter, and R. A. J. Janssen, Phys. Rev. B **70**, 045202 (2004).